Atmospheric Environment 246 (2021) 118131

Contents lists available at ScienceDirect

Atmospheric Environment

journal homepage: http://www.elsevier.com/locate/atmosenv

Modelling air quality during the EXPLORE-YRD campaign – Part I. Model performance evaluation and impacts of meteorological inputs and grid resolutions

Xueying Wang [a], Lin Li [a], Kangjia Gong [a], Jianjiong Mao [a], Jianlin Hu [a,*], Jingyi Li [a], Zhenxin Liu [a], Hong Liao [a], Wanyi Qiu [b], Ying Yu [b], Huabin Dong [b], Song Guo [b], Min Hu [b], Liming Zeng [b], Yuanhang Zhang [b,c]

[a] *Jiangsu Key Laboratory of Atmospheric Environment Monitoring and Pollution Control, Collaborative Innovation Center of Atmospheric Environment and Equipment Technology, Nanjing University of Information Science & Technology, Nanjing, 210044, China*

[b] *State Key Joint Laboratory of Environmental Simulation and Pollution Control, College of Environmental Sciences and Engineering, Peking University, Beijing, 100871, China*

[c] *CAS Center for Excellence in Regional Atmospheric Environment, Chinese Academy of Science, Xiamen, 361021, China*

HIGHLIGHTS

- Air quality is predicted using WRF/CMAQ for the EXPLORE-YRD campaign.
- ERA5 reanalysis data yield slightly better PM2.5 predictions than FNL, but both underpredict the high PM2.5 events.
- O3 performance is similar with ERA5 and FNL.
- Grid resolution is not a key factor for modelling PM2.5 and O3 in YRD.

ARTICLE INFO

Keywords:
EXPLORE-YRD
Reanalysis data
Grid resolution
Model performance
PM2.5
O3

ABSTRACT

The EXPeriment on the eLucidation of the atmospheric Oxidation capacity and aerosol foRmation and their Effects in the Yangtze River Delta (EXPLORE-YRD) campaign was carried out between May and June 2018 at a regional site in Taizhou, China. The EXPLORE-YRD campaign helped construct a detailed air quality model to understand the formation of O_3 and $PM_{2.5}$ further, identify the key sources of elevated air pollution events, and design efficient emission control strategies to reduce O_3 and $PM_{2.5}$ pollution in YRD. In this study, we predicted the air quality during the EXPLORE-YRD campaign using the Weather Research and Forecasting/Community Multiscale Air Quality modelling system (WRF/CMAQ) and evaluated model performance on O_3 and $PM_{2.5}$ concentrations and compositions. **Air quality was predicted using two sets of reanalysis data—**NCEP Final (FNL) Operational Global Analysis **and ECMWF Reanalysis v5.0 (ERA5)—and three horizontal resolutions of 36, 12, and 4 km.** The results showed that $PM_{2.5}$ concentration was generally under-predicted using both the FNL and ERA5 data. ERA5 yielded slightly higher $PM_{2.5}$ predictions during the EXPLORE-YRD campaign. Both reanalysis data sets under-predicted the high $PM_{2.5}$ pollution processes on 29–30 May 2018, indicating that reanalysis data is not essential for under-predicting extreme $PM_{2.5}$ pollution processes. The performance of O_3 was similar in both the reanalysis data sets, because O_3 is mostly sensitive to temperature predictions and FNL and ERA5 yielded similar temperature results. Although the average performance of $PM_{2.5}$ and O_3 predictions yielded by FNL and ERA5 was similar, large differences were observed in certain locations on specific days (e.g. in Hangzhou between 29 May and June 6, 2018 and in Hefei on 1–3 June 2018). Therefore, the choice of reanalysis data could be an important factor affecting the predictions of $PM_{2.5}$ and O_3, depending on locations and episodes. Comparable results were obtained using predictions with different horizontal resolutions, indicating that grid resolution was not crucial for determining the model performance of both $PM_{2.5}$ and O_3 during the campaign.

* Corresponding author.
E-mail address: jianlinhu@nuist.edu.cn (J. Hu).

https://doi.org/10.1016/j.atmosenv.2020.118131
Received 26 March 2020; Received in revised form 22 November 2020; Accepted 2 December 2020
Available online 8 December 2020

1. Introduction

The Yangtze River Delta (YRD) region is located in East China and has experienced severe regional haze pollution and photochemical smog pollution due to rapid economic growth and increase in urban agglomerations in recent decades (Li et al., 2015a, 2016, 2019; Ma et al., 2019; Ming et al., 2017; Shu et al., 2016, 2017, 2019, 2020; Wang et al., 2015). Particulate matter with diameters equal to or less than 2.5 μm ($PM_{2.5}$) and ozone (O_3) are the two major air pollutants in YRD (Fan et al., 2020; Pui et al., 2014; Wang et al., 2014) and have attracted increased attention in China (Guo et al., 2014, 2020; Lu et al., 2019). Several studies have been conducted to investigate the spatial and temporal variations (Hu et al., 2014; Wang et al., 2014, 2017) and recent trends (Ma et al., 2019; Pan et al., 2017) in $PM_{2.5}$ and O_3 in this region. Ma et al. (2019) pointed out that $PM_{2.5}$ shows a downward trend, but O_3 increases. Moreover, a few severe pollution events in YRD have been studied to understand the characteristics, sources, and impact factors of $PM_{2.5}$ and O_3 (Li et al., 2015a, 2016, 2019; Shen et al., 2015; Zhang et al., 2019). The major anthropogenic sources of high O_3 pollution in summer in this region include industrial combustion, industrial processes, and mobile sources (Li et al., 2015a, 2016, 2019). Studies by Shen et al. (2015) and Zhang et al. (2019) suggested that during heavy haze events in the YRD region, nitrate (NO_3^-) dominates over sulphate (SO_4^{2-}), dissimilar to the North China Plain region. Studies have also found that meteorological conditions and regional transport can play an important role in the development of pollutants, such as cold fronts that bring air pollutants from polluted upstream areas (Kang et al., 2019) and high-pressure systems that are favourable for the accumulation of pollutants in YRD (Shu et al., 2017).

To understand the formation of O_3 and $PM_{2.5}$ in YRD, the EXPeriment on the eLucidation of the atmospheric Oxidation capacity and aerosol foRmation, and their Effects in the Yangtze River Delta (EXPLORE-YRD) campaign was carried out between May and June 2018 at a regional site in Taizhou, Jiangsu Province, China. The comprehensive measurements of O_3, CO, NOx, and SO_2, and detailed VOCs were made during the campaign. PM concentrations, its chemical composition, and relevant precursors were also measured. Meteorological conditions were monitored, including temperature at a height of 10 m (T2), relative humidity (RH), wind speed (WS) and direction (WD) at a height of 10 m, and planetary boundary layer height (PBL). These data provided strong support to build a detailed air quality model (AQM) in order to understand the formation of O_3 and $PM_{2.5}$ further, identify the key sources that cause the elevated air pollution events, and design efficient emission control strategies to reduce O_3 and $PM_{2.5}$ pollution in YRD.

The Weather Research and Forecasting Model (WRF)/Community Multiscale Air Quality (CMAQ) modelling system was applied to simulate air quality using the data collected during the EXPLORE-YRD campaign. The WRF/CMAQ modelling system has been previously applied to study air quality in different regions of China and has provided valuable information on the formation mechanisms, potential impacts of emission control strategies and climate change, and health impacts. For example, Hu et al. (2016b) evaluated the performance of the WRF/CMAQ model on $PM_{2.5}$ and O_3 in China from 2013 to 2014 and found that the model could successfully reproduce the O_3 and $PM_{2.5}$ concentrations in most cities in different seasons. Yang et al. (2019) used the CAMQ model and demonstrated that poor meteorological conditions were the primary reason for air quality deterioration in the winter of 2015 in Xi'an. Ding et al. (2019) used CMAQ to evaluate the response of O_3 pollution to emissions and meteorological changes during the warm seasons of 2013 and 2017 and concluded that MDA8 O_3 was significantly influenced by anthropogenic emissions and meteorological variations. Zhang et al. (2020) used the positive matrix factorisation method and CMAQ to estimate the source contribution of sulphur and nitrogen's wet deposition on Mt. Emei from 2017 to 2019, revealing that the emissions within and outside the Sichuan Basin were substantial. Combining field observations and CMAQ simulation characterisation, Liu et al. (2020a) analysed the seasonal characteristics of aerosol in Beijing and observed increases in the relative abundances of the major aerosol components (i.e. SO_4^{2-}, NO_3^-, organic carbon (OC), and water-soluble organic carbon) when RH exceeded approximately 65% in winter. Hu et al. (2017a) predicted the impact of different future power generation plans in China on air quality using the CMAQ model. Uncertainties in the emission inventory can significantly impact the model predictions. For example, Huang et al. (2011) estimated that emission inventory in the YRD region has an overall uncertainty of ±19.1%, ±27.7%, ±167.6%, ±133.4%, and ±112.8% for SO_2, NOx, $PM_{2.5}$, VOCs, and NH_3, respectively. Hu et al. (2017d) evaluated CMAQ model performance using four different emission inventories in China and found that, in general, model performance in more developed regions, such as the YRD region, is better than that in western China. Wang et al. (2020) developed five biogenic emission cases with different land cover input and emission factors and evaluated their impacts on air quality in YRD. Their results indicated that the isoprene emissions in July could be underestimated by 37% in southern YRD when using the default emission factors.

Even though the models performed satisfactorily in the aforementioned studies, a few factors were identified to substantially impact the accuracy of model prediction, besides the uncertainties associated with emission inputs (the bias in the meteorological inputs and the model resolutions). Meteorological conditions seemed to play a key role in affecting the O_3 and $PM_{2.5}$ pollution. The meteorological inputs required by the AQM studies are generally created using either the diagnostic method (derived from intensive meteorological observations) or, more often, prognostic methods (predicted by meteorological models, such as WRF) (Hu et al., 2010). Bias in WRF predicted wind speeds (biased low for low wind speeds, and biased high for high wind speeds) and was strongly correlated with the bias in the predicted PM concentrations (Hu et al., 2015). Reanalysis data, used as initial and boundary conditions for WRF simulations, also seemed to affect the accuracy of meteorological predictions. For example, Monk et al. (2019) compared WRF predictions in Sydney, Australia, using NCEP Final (FNL) Operational Global Analysis and **European Centre for Medium-Range Forecasting (ECMWF) Reanalysis (ERA) Interim** reanalysis data and found that model results using FNL were better than those of ERA-Interim. Another study by Tao et al. (2020) reported similar findings from Beijing. The impact of different meteorological initial and boundary conditions (GFS and Reanalysis II) on the model was evaluated by (Ritter et al., 2012), and one of their conclusions was that the GFS model had a higher resolution, leading to slightly better results.

Grid resolution was another factor commonly reported in air quality modelling. Many studies have been conducted to investigate the influence of resolution on model simulations in different regions. For instance, Pan et al. (2017) compared WRF meteorology fields at 1 and 4 km resolution and found no significant differences in temperature, wind, PBL, and cloud fraction between the models. Tao et al. (2020) determined that with an increased resolution from 3 to 1 km, the mean bias (MB) of T2 reduced from 2 °C to 1.7 °C, and the 1 km resolution simulation represented meteorological field magnitudes and temporal trends better. Arunachalam et al. (2006) indicated that no significant difference existed when predicting simulated air quality using 4 and 12 km resolutions, and there was an insignificant difference between 4 and 36 km resolution models in North Carolina. Jiang and Yoo (2018) showed that the simulation results at both 4 and 12 km resolutions reproduced the $PM_{2.5}$ measurements, but the predictions at 12 km resolution generally showed better results and were much less computationally intensive than those at the 4 km resolution. Liu et al. (2020b) found that model resolution could cause a substantial difference in the population exposure and health burden estimates of O_3 in Nanjing. The inconsistent findings among these studies indicate that the impact of grid resolution needs to be studied further using different model practices.

The purpose of this study is to evaluate the performance of the WRF/

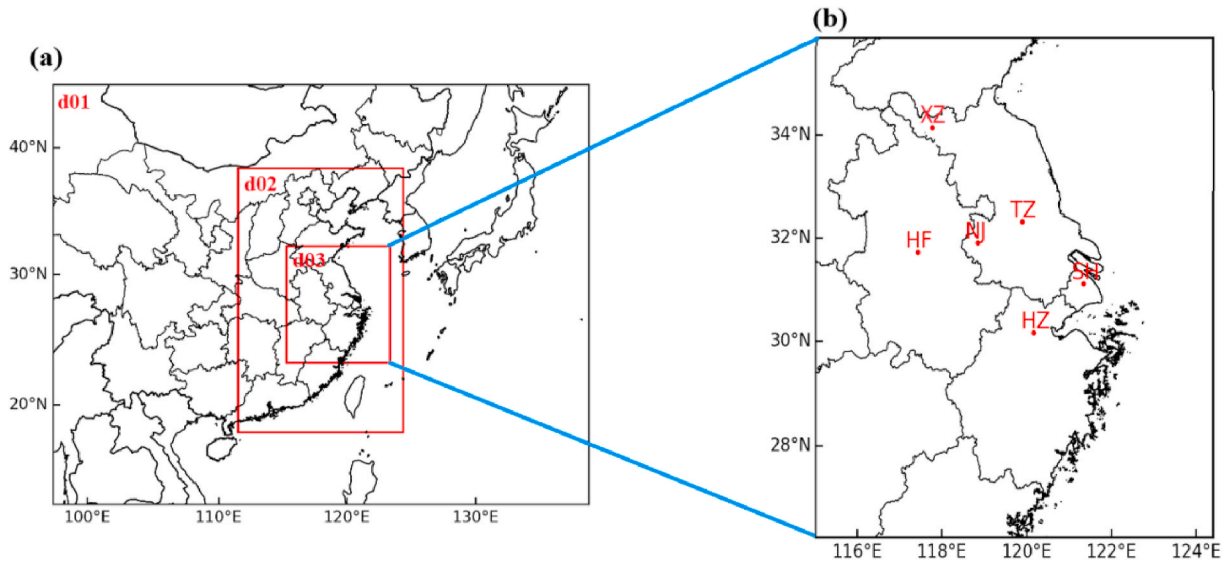

Fig. 1. WRF/CMAQ domain configuration: (a) three domains for simulations and (b) the geographical distribution of six cities in the Yangtze River delta (including TZ: Taizhou, HZ: Hangzhou, NJ: Nanjing, SH: Shanghai, XZ: Xuzhou, HF: Hefei).

CMAQ air quality modelling system for the key gas- and particulate-phase pollutants in the YRD region during the EXPLORE-YRD campaign. Here, we also discuss the impacts of different meteorological reanalysis data and grid resolutions on CMAQ performance in the YRD region. The validation of the model results should provide the source apportionment and chemical evolution of O_3 and $PM_{2.5}$ for the subsequent modelling studies as well as the emission control strategy analysis for the YRD region.

2. Methods

2.1. Meteorological simulations

Meteorological conditions were simulated using the WRF model version 4.0 with two different sets of reanalysis data—FNL and ERA5. The 6 h FNL Operational Global Reanalysis data are the NCEP data from the U.S. National Centre for Atmospheric Research (NCAR), with a spatial resolution of 1.0 ° × 1.0 ° (https://rda.ucar.edu/datasets/ds083.2/). These data were obtained from the Global Data Assimilation System (GDAS), which continuously collects observational data from the Global Telecommunications System (GTS) and other sources for many analyses. The collected parameters include such meteorological parameters as ground pressure, sea level pressure, geopotential temperature, sea surface temperature, soil temperature, ice cover, relative humidity, U wind, and V wind. The FNL data have been widely used in many studies to simulate meteorological conditions and air quality in different regions. For example, Yusoff et al. (2019) applied the FNL meteorological data to calculate the backward trajectory using the hybrid single-particle Lagrangian integral trajectory model and evaluated the spatio-temporal distribution characteristics of ground-level O_3 in Malaysia at night. Nguyen et al. (2019) assessed the impact of future potential climate change on $PM_{2.5}$ and O_3 air quality in Southeast Asia. Kota et al. (2018) utilised the NCEP FNL data to drive the WRF/CMAQ model and simulated gas and particulate air pollutants in India. The FNL data have also been commonly used to drive WRF and air quality studies in China. For instance, Zhang et al. (2019) studied the $PM_{2.5}$ pollution event process in Chinese coastal cities. Wang et al. (2019b) simulated and analysed the effects of ship emissions on O_3 in YRD, China, using the WRF-Chem model. Wang et al. (2019a) investigated the response of $PM_{2.5}$ and O_3 concentrations to changes in meteorological conditions and emissions in China using the WRF/CMAQ model.

ERA5 is the fifth generation ECMWF atmospheric global climate reanalysis data and is based on the Integrated Forecasting System (IFS) Cy41r2, which was operational in 2016 (Hersbach et al., 2020). The ECMWF ERA5 reanalysis data in WRF have the following specifications: a horizontal resolution of 0.3 × 0.3 and a temporal resolution of 6 h. It includes atmospheric parameters (e.g. air temperature, pressure, and wind at different altitudes) and surface parameters (e.g. rainfall, soil moisture content, ocean surface temperature, and wave height) updated ((C3S), 2017). Tao et al. (2020) used ERA5 as the meteorological driver and analysed the impact of model resolution on predicted meteorological conditions and air quality. They also simulated human exposure to $PM_{2.5}$ and O_3 in Beijing, China.

Table 1
WRF physics options.

Physics Option	D01 (36 km)& D02 (12 km)&D03 (4 km)
Microphysics	Thompson scheme
Longwave radiation	rrtmg scheme
Shortwave radiation	rrtmg scheme
Surface layer	Revised MM5 Monin-Obukhov scheme
Land surface	Unified Noah land-surface mode
Planetary Boundary Layer	YSU scheme
Cumulus Parameterization	Grell-Freitas ensemble scheme

Herein, the meteorological fields were simulated using the FNL and ERA5 reanalysis data between 17 May and June 17, 2018. The WRF v4.0 model with the research core was used for this study. The spin-up of the model equalled 2 d. Three nesting domains with horizontal resolutions of 36, 12, and 4 km were used. The 36 km domain covered China and the surrounding countries with 137 × 107 grids; the 12 km domain covered eastern China with 127 × 202 grids; and the 4 km domain covered the entire YRD region with 238 × 268 grids (Fig. 1). The major physics options are listed in Table 1.

2.2. Air quality simulations

An updated version of CMAQ v5.0.2 was applied to simulate air quality from May to June 2018. The update was made in the SAPRC11 gas-phase photochemical mechanism model (Carter and Heo, 2012), where a more detailed isoprene oxidation scheme was used (Hu et al., 2017c). Updates were also made in the aerosol treatment processes to include (1) the heterogeneous formation of NO_3^- and SO_4^{2-}, following the methods described by Ying et al. (2014), and (2) the heterogeneous

Table 2
Meteorological simulation effects of 6 cities in the Yangtze River Delta region during the EXPLORE-YRD campaign. (OBS: the observed average; FNL and ERA5: the simulated averages of FNL and ERA5, respectively; MB: mean bias; ME: mean error; RMSE: root mean square error).

			Hangzhou		Hefei		Nanjing		Shanghai		Taizhou		Xuzhou		Bench-mark
T2 °C	OBS		24.58		24.17		23.89		24.24		23.18		25.04		
	FNL	ERA5	25.80	26.19	26.26	26.48	23.83	24.36	22.92	23.59	22.46	22.87	25.92	25.62	
	MB		**1.22**	**1.61**	**2.09**	**2.31**	−0.06	0.47	**−1.32**	**−0.65**	**−0.72**	−0.31	**0.87**	**0.57**	≤±0.5
	ME		1.50	1.81	**2.21**	**2.39**	1.16	1.15	1.53	1.36	1.35	1.38	1.30	1.25	≤2.0
	RMSE		1.90	2.20	2.49	2.65	1.41	1.41	1.81	1.65	1.66	1.77	1.60	1.52	
RH %	OBS		78.16		77.60		77.23		74.42		74.38		62.90		
	FNL	ERA5	63.23	63.89	55.48	59.04	66.46	68.23	71.22	70.01	69.08	72.45	46.83	51.57	
	MB		−14.93	−14.27	−22.12	−18.56	−10.77	−9.00	−3.20	−4.40	−5.29	−1.92	−16.08	−11.33	
	ME		17.84	16.46	24.61	20.37	14.57	12.72	10.97	11.68	10.60	10.38	18.12	17.52	
	RMSE		20.60	18.86	26.26	22.73	16.89	15.13	13.88	13.80	13.53	13.05	20.76	19.59	
WS m/s	OBS		2.33		2.26		2.39		3.31		2.37		1.81		
	FNL	ERA5	2.25	2.38	2.27	2.31	2.89	2.90	0.74	0.81	3.08	2.96	2.99	3.11	
	MB		−0.07	0.05	0.01	0.05	0.50	**0.51**	**−2.57**	**−2.51**	**0.71**	**0.59**	**1.18**	**1.30**	≤±0.5
	ME		0.82	0.84	1.49	1.66	0.78	0.88	**2.57**	**2.51**	1.64	1.64	1.35	1.32	≤2.0
	RMSE		1.08	1.09	1.83	1.99	0.97	1.13	**2.76**	**2.67**	**2.01**	**2.02**	1.50	1.52	≤2.0
WD °	OBS		137.31		153.84		145.66		136.84		139.09		157.10		
	FNL	ERA5	148.37	149.17	141.31	159.00	123.16	128.89	210.70	141.28	135.14	129.32	155.68	156.08	
	MB		**11.06**	**11.86**	**−12.53**	5.16	**−22.49**	**−16.77**	**73.86**	4.44	−3.96	−9.77	−1.42	−1.02	≤±10
	ME		**65.88**	**63.63**	**36.15**	**33.84**	**36.80**	**36.23**	**133.04**	**96.37**	**36.78**	**36.84**	**41.70**	23.19	≤±30
	RMSE		118.09	115.35	65.62	51.17	53.47	54.91	162.91	125.12	74.71	61.64	85.87	28.85	

formation of secondary organic aerosol SOA from dicarbonyls, isoprene epoxy diol, and methacrylic acid epoxide, as described in (Hu et al., 2017c; Li et al., 2015b; Ying et al., 2015). The updated CMAQ v5.0.2 model with the 36 km horizontal resolution was applied to simulate air quality in 2013 in China (Hu et al., 2016b, 2017b). The model performance of $PM_{2.5}$ and O_3 was validated against ambient measurements, with an average mean fractional bias of −0.35, mean fractional error of 0.52 for daily $PM_{2.5}$, mean normalised bias of 0.34, and mean normalised error of 0.49 for daily maximum O_3 in over 60 cities in China. More details on the CMAQ updates and configurations can be found in Hu et al. (2016), Hu et al. (2017b), and references therein.

The simulation period was set from May to June 2018. A total of 18 vertical layers were used, among which 8 layers were distributed below a height of 1 km with a high resolution to describe the atmospheric boundary layer structure in detail, whereas the height of the ground layer was approximately 35 m. The Multi-resolution Emission Inventory for China (MEIC, 2016) (http://www.meicmodel.org) was used to retrieve the anthropogenic emissions and biogenic emissions generated using the Model for Emissions of Gases and Aerosols from Nature (MEGAN) version 2.1 (Guenther et al., 2012). The chemical reaction mechanism of the gas phase was SAPRC11, and the aerosol reaction mechanism was Aero6. Other configurations followed the description provided in Hu et al. (2016).

2.3. Measurement data and evaluation metrics

The EXPLORE-YRD campaign provided $PM_{2.5}$, O_3, and meteorological data at various Taizhou monitoring sites. The sampling site was located at Taizhou meteorological radar station (lat 32°35′ N, long 119°57' E), Jiangsu Province, with a sampling port located 3 m above the ground. The weather data were provided directly from the site from 14 May to June 18, 2018, with a temporal resolution of 60 s. Temperature, humidity, wind direction, and wind speed were processed for a time resolution of 1 h. Pollutant concentration was collected from 17 May to June 17, 2018 for a total of 31 d. $PM_{2.5}$ with a time resolution of 60 s was obtained using a TEOM 1400 ab aerosol mass concentration monitor. EC/OC was analysed using the online EC/OC analyser, with a temporal resolution of 30 min (Hu et al., 2012). SO_4^{2-}, NO_3^-, and NH_4^+ were acquired using an online collection and analysis system of water-soluble ions of gas/aerosol with a time resolution of 30 min (Dong et al., 2012). The pollutant data mentioned above were calculated to obtain hourly and daily observations. O_3 was measured using an ultraviolet photometric analyser (Model 49i, Thermo Fischer Scientific, USA), with a time resolution of 60 s. Hourly O_3 concentrations were then averaged, and the daily maximum 8 h O_3 concentrations (O_3-8 h) were calculated for each day. The processed observational data were compared with the simulated data.

In addition to the ambient data measured at the Taizhou station, air quality and meteorological data were collected in five other major cities in YRD (i.e., Shanghai, Nanjing, Hangzhou, Hefei, and Xuzhou), with their locations depicted in Fig. 1. Hourly $PM_{2.5}$ and O_3 concentrations in the five cities from May to June 2018 were downloaded from the website of the China National Environment Monitoring Centre (http://113.108.142.147:20035/emcpublish). Meteorological observation data were obtained from the National Centres for Environmental Prediction (ftp://ftp.ncdc.noaa.gov/pub/data/noaa/).

The statistical metrics of the mean bias (MB), mean error (ME), and root mean square error (RMSE) were calculated to evaluate the meteorological predictions as follows:

$$\mathrm{MB} = \frac{1}{N}\sum_{i=1}^{N}(M_i - O_i), \tag{1}$$

$$\mathrm{ME} = \frac{1}{N}\sum_{i=1}^{N}|M_i - O_i|, \tag{2}$$

$$\mathrm{RMSE} = \left[\frac{1}{N}\sum_{i=1}^{N}(M_i - O_i)^2\right]^{1/2}, \tag{3}$$

where N is the total number of data points; M_i is the ith predicted value; and O_i is the ith observed value. The model performance benchmarks of these metrics for the temperature at 2 m (T2), wind speed at 10 m (WS), and wind direction at 10 m (WD), as proposed by Emery et al. (2001), are listed in Table 2.

The statistical metrics of normalised mean deviation (NMB) and normalised mean error (NME) were calculated to evaluate the air quality predictions as follows:

$$\mathrm{NMB} = \frac{\sum_{i=1}^{N}(M_i - O_i)}{\sum_{i=1}^{N}O_i}, \tag{4}$$

$$\mathrm{NME} = \frac{\sum_{i=1}^{N}|M_i - O_i|}{\sum_{i=1}^{N}O_i}. \tag{5}$$

The model performance benchmarks of NMB and NME for $PM_{2.5}$ and O_3, as suggested by Emery et al. (2017), are listed in Table 3.

Table 3
Model performance of $PM_{2.5}$ and O_3-8 h concentrations in 6 cities in the Yangtze River Delta region from May to June 2018 (OBS: the observed average; FNL and ERA5: the simulated averages of FNL and ERA5, respectively; NMB: normalised mean bias; NME: the normalised mean error).

			Hangzhou		Hefei		Nanjing		Shanghai		Taizhou		Xuzhou		Bench-mark
$PM_{2.5}$ May–Jun $\mu g/m^3$	OBS		35.96		44.36		36.94		43.14		49.51		43.62		
	FNL	ERA5	30.95	31.55	47.58	47.41	39.95	39.62	27.76	28.11	37.70	39.09	39.31	38.57	
	NMB		−14%	−12%	7%	7%	8%	7%	**−36%**	**−35%**	−24%	−21%	−10%	−12%	<±30%
	NME		34%	35%	29%	35%	36%	26%	42%	41%	32%	31%	34%	30%	<50%
O_3 May–Jun $\mu g/m^3$	OBS		145.60		148.37		154.37		142.22		161.56		172.19		
	FNL	ERA5	129.93	133.58	130.15	138.12	123.62	129.20	110.40	113.25	137.70	138.18	139.09	144.08	
	NMB		−11%	−8%	−12%	−7%	**−20%**	**−16%**	**−22%**	**−20%**	−15%	−14%	**−19%**	**−16%**	≤±15%
	NME		27%	**31%**	24%	19%	25%	22%	24%	23%	22%	21%	24%	19%	≤30%

3. Results

3.1. Evaluation of meteorological and air quality predictions using FNL

3.1.1. Meteorological predictions

Table 2 shows model performance for the temperature at 2 m (T2), relative humidity at 2 m (RH), WS, and WD, with the FNL reanalysis data during the modelling period (Table 2 also includes the results obtained using the ERA5 data, which are discussed in Section 3.2). Using the FNL reanalysis data, T2 was generally over-predicted in Hangzhou, Hefei, and Xuzhou and underestimated in Nanjing and Taizhou. The MB value of T2 in Taizhou was - 0.72 °C and exceeded the benchmark (±0.5 °C), whereas the ME value was 1.35 °C and stayed within the benchmark (2.0 °C). The MB (- 0.06 °C) and ME (1.16 °C) values in Nanjing met the benchmark. The MB values in the other five cities (Hangzhou 1.22 °C, Hefei 2.09 °C, Shanghai - 1.32 °C, Taizhou - 0.72 °C, Xuzhou 0.87 °C) did not meet the benchmark, while ME satisfied the benchmark, except in Hefei (2.21 °C). The MB values in all analysed cities ranged from - 0.06 °C to 2.4 °C and were lower than the average values across China from 2013, as reported by Hu et al. (2016a), although the ME values were slightly higher in this study. No benchmarks were suggested for the MB and ME values of RH. RH was underestimated in all the cities, consistent with the study by Hu et al. (2016a). The average observed WS ranged from 1.81 to 3.31 m s^{-1}, indicating relatively calm conditions during the campaign. Overall, WS was over-predicted by WRF with FNL, except in Shanghai and Hangzhou, but the predictions generally agreed well with the observations, as indicated by the MB, ME, and RMSE values. The over-predictions of low wind speeds by WRF, especially for wind speeds of less than 3 m s^{-1}, have been previously reported (Angevine et al., 2012; Fast et al., 2014; Hu et al., 2015, 2016a; Michelson et al., 2010). The ME values met the benchmark in five cities, except Shanghai (2.57 m s^{-1}). The RMSE values met the benchmark in four cities, except Shanghai (2.76 m s^{-1}) and Taizhou (2.01 m s^{-1}), whereas MB met the benchmark only in Hangzhou (−0.07 m s^{-1}), Hefei (0.01 m s^{-1}), and Nanjing (0.50 m s^{-1}). The prevailing WD during the campaign was from the southeast, as indicated by the observations. WRF predicted WD properly in Taizhou (- 3.96°) and Xuzhou (- 1.42°) but presented a 10°–80° bias in the other four cities. The ME values in all cities were slightly greater than the benchmark, especially in Hangzhou (65.88°) and Shanghai (133.04°). Similar performance of WD was reported by Hu et al. (2016a).

Fig. 2 shows the comparison of observed and predicted hourly T2, RH, WS, WD, and PBL in Taizhou during the campaign. The diurnal and daily variations of T2 and RH reproduced WS well, showing no obvious diurnal and daily variations in Taizhou, whereas the WRF model over-predicted WS. Previous studies have pointed out that the WRF model tends to over-predict slow winds (Gsella et al., 2014; Hu et al., 2015; Zhang et al., 2014). In most cases, easterly winds (including east, northeast, and southeast) predominated in Taizhou, and the model predicted WD values agreed well with the observations. Generally, PBL predicted by ERA5 was slightly lower than that by FNL, especially during the peak period.

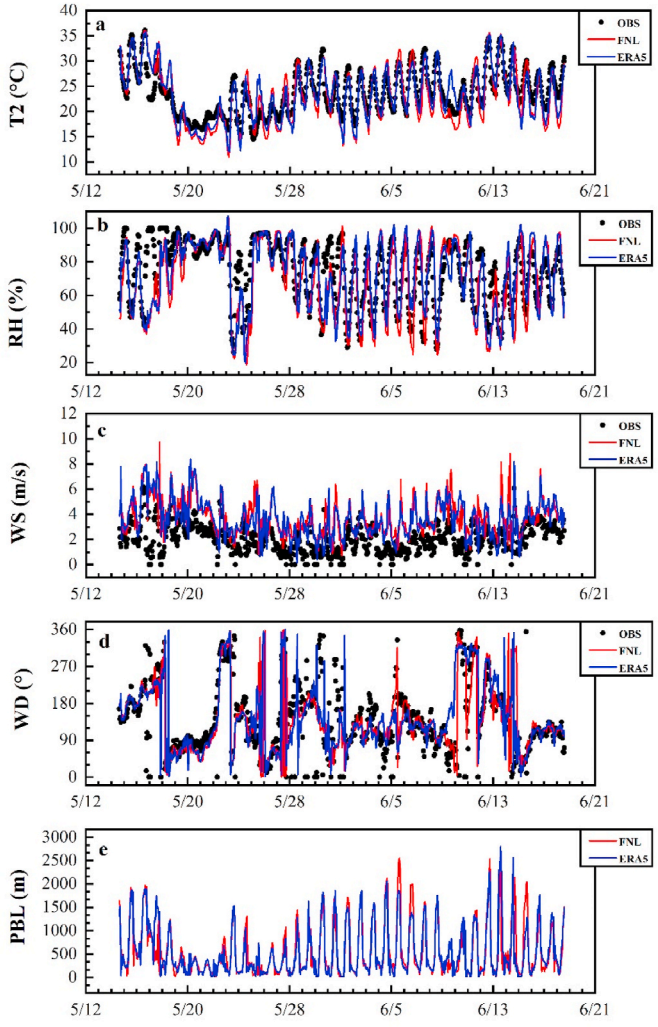

Fig. 2. Comparison of temperature at 2 m (T2), relative humidity (RH), wind speed (WS) at 10 m, wind direction (WD) at 10 m, and planetary boundary layer height (PBL) simulated by FNL and ERA5 meteorological data and observation values for Taizhou during the EXPLORE-YRD campaign.

3.1.2. Air quality predictions

Table 3 shows CMAQ model performance for $PM_{2.5}$ and O_3-8 h in the six cities with the predicted meteorological conditions using FNL (and ERA5, as discussed in Section 3.2). In general, $PM_{2.5}$ concentrations predicted using FNL were similar to the observed concentrations in the five cities, except in Shanghai (- 36%). The NME (50%) and NMB

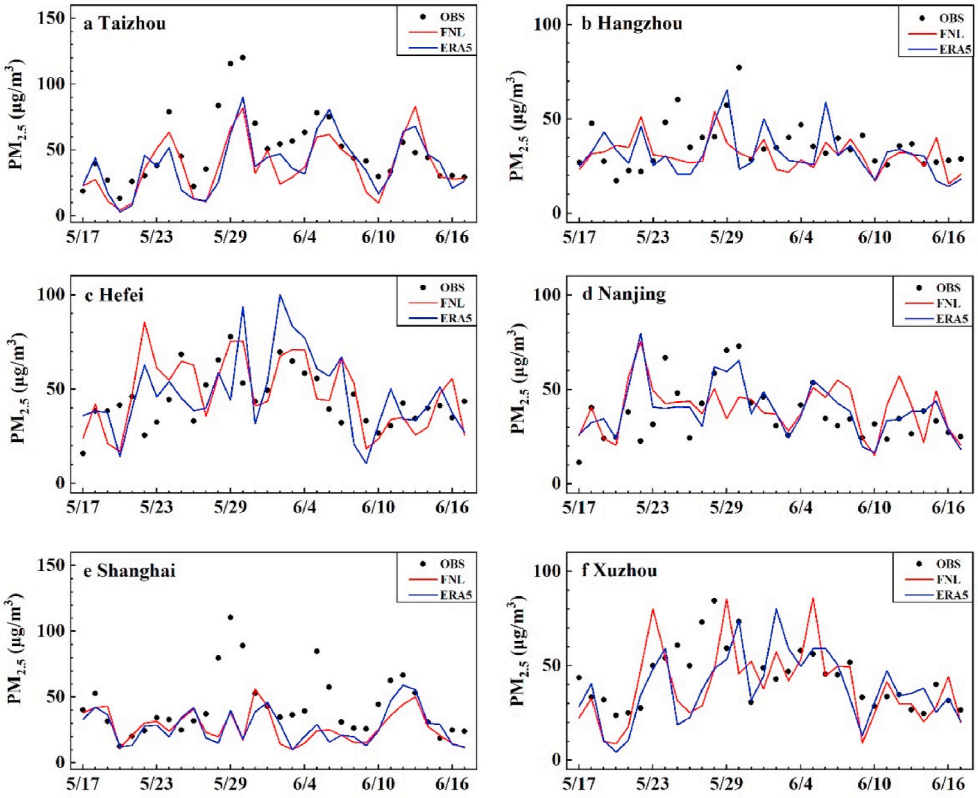

Fig. 3. Comparison of $PM_{2.5}$ concentrations and observations simulated using FNL and ERA5 meteorological data in six cities.

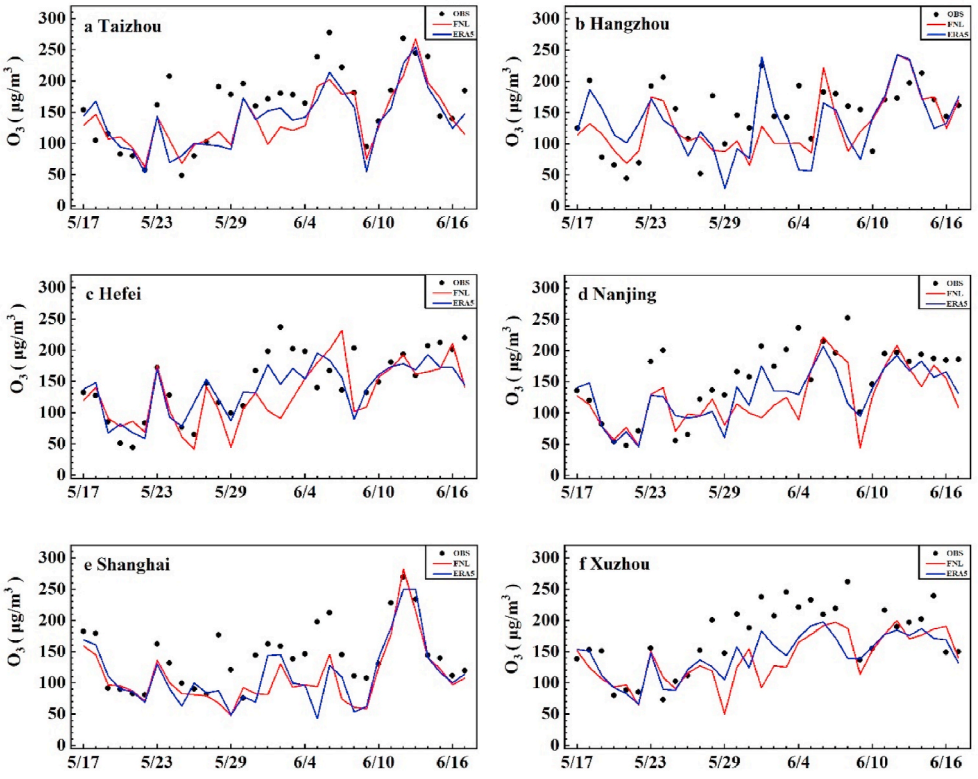

Fig. 4. Comparison of MAD8h O_3 concentrations and observations simulated using FNL and ERA5 meteorological data in six cities.

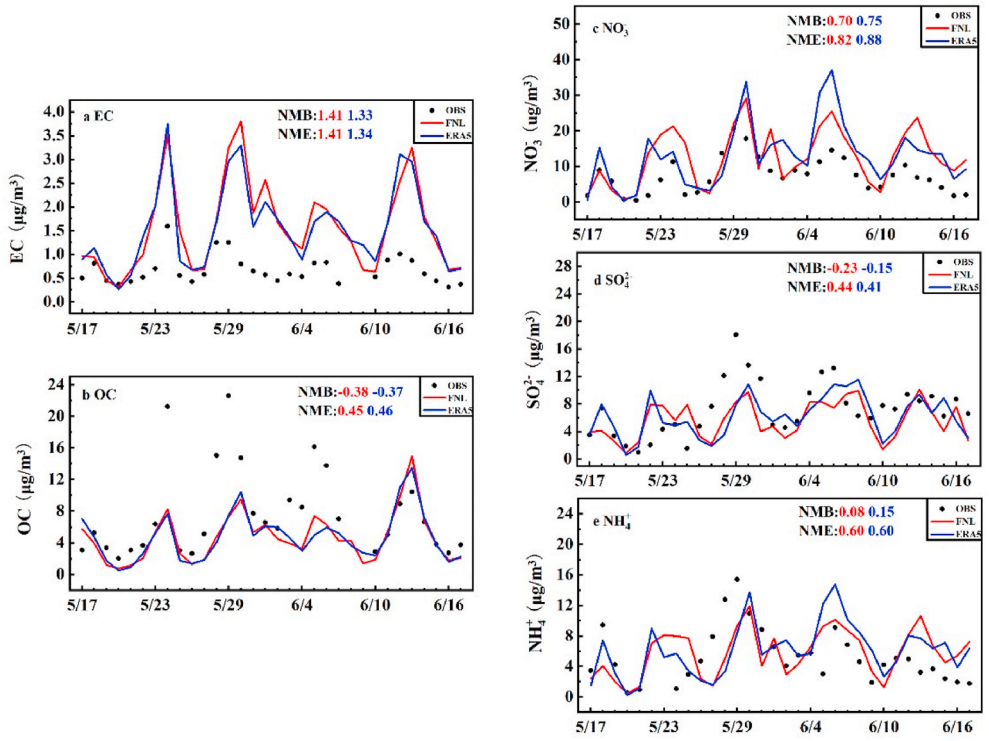

Fig. 5. Comparison of $PM_{2.5}$ component concentrations and observations simulated using FNL and ERA5 meteorological data in Taizhou.

(±30%) values in the other five cities met the benchmark. Most NMB values were negative, except in Hefei (7%) and Nanjing (8%), indicating that the $PM_{2.5}$ total mass was under-predicted by CMAQ. The performance of O_3-8 h with FNL was worse than the performance of $PM_{2.5}$ with FNL. The NME values satisfied the O_3-8 h benchmark (±15%) in all cities, and the NMB value satisfied the O_3-8 h benchmark (30%) in Hangzhou (11%), Hefei (- 12%), and Taizhou (- 15%) and was only slightly higher than the benchmark of 15% in Nanjing (- 20%), Shanghai (- 22%), and Xuzhou (- 19%). O_3-8 h was also under-predicted in most cities, as indicated by the small negative values.

Figs. 3 and 4 illustrate the time series of predicted and observed 24 h $PM_{2.5}$ and O_3-8 h concentrations in the six cities, respectively. $PM_{2.5}$ concentrations were consistently under-predicted by CMAQ with the FNL meteorology. The observed $PM_{2.5}$ exhibited strong day-to-day variations during the campaign, with low concentrations of less than 10 μg/m^3 and high concentrations exceeding 100 μg/m^3 (29–30 May 2018). The CMAQ predictions with FNL did not capture the strong day-to-day variations in $PM_{2.5}$ concentration. The high $PM_{2.5}$ concentrations were largely missed in the predictions. Compared to $PM_{2.5}$, the performance of O_3-8 h was better, although the model predictions were lower than the actual observations and missed the high O_3 values that occurred in early June 2018.

Further model evaluation of $PM_{2.5}$ components was performed using the data measured during the campaign in Taizhou. Fig. 5 shows the comparison of predicted and observed SO_4^{2-}, NO_3^-, NH_4^+, OC, and EC concentrations. With the FNL reanalysis data, the predicted EC concentrations agreed well with the observed values, with an NMB of 141% and an NME of 141%. The predicted NO_3^- concentrations were higher than the observed values, with an NMB of 70% and an NME of 82%. All other components were under-predicted, with an NMB of - 23%, - 54%, and - 38% for SO_4^{2-}, NH_4^+, and OC, respectively, and an NME of 44%, 67%, and 45% for SO_4^{2-}, NH_4^+, and OC, respectively. The high $PM_{2.5}$ pollution on 29–30 May 2018 was largely due to the contribution of SO_4^{2-}, NO_3^-, NH_4^+, and OC, but the model with FNL did not capture the peak values.

3.2. Impact of reanalysis data on meteorological and air quality predictions

To analyse the impact of the reanalysis data on air quality predictions, another set of WRF/CMAQ simulations was conducted using the ERA5 reanalysis data with the same model configurations and emissions. The statistical results of meteorological predictions using ERA5 are shown in Table 2. For T2, ERA5 yielded slightly higher predictions, except in Xuzhou, compared to those with FNL. The MB values indicated that the predictions by ERA5 were better than by FNL, meeting the benchmark (±0.5 °C) in three more cities, i.e. Shanghai (- 0.65 °C), Taizhou (- 0.31 °C), and Xuzhou (0.57 °C). The ME values were similar between the two reanalysis datasets. ERA5 also yielded better RH predictions, with smaller negative MB values in most cities, except for Shanghai's higher MB (- 4.40%) and ME (11.68%). The WS values predicted with ERA5 were also over-predicted, and the over-prediction was more than that with FNL, except for Taizhou. In general, the T2 and RH simulation values obtained with the ERA5 dataset were closer to the actual observations, while the WS and WD simulation results were better using the FNL dataset. Our results are in line with the findings of Tao et al. (2020).

The impact of reanalysis data on $PM_{2.5}$ and O_3-8 h are presented in Figs. 3 and 4. The predicted O_3-8 h concentrations driven by the two reanalysis data were comparable, and the predictions using ERA5 were generally higher than those using FNL. The $PM_{2.5}$ concentrations obtained using the ERA5 data set showed the same change. This is also reflected in the NMB and NME values listed in Table 2. Compared to FNL, the improvement in the $PM_{2.5}$ prediction by ERA5 was mainly due to the improved predictions of SO_4^{2-}. NMB was improved from - 23% to - 15% for SO_4^{2-}, and NME was improved from 44% to 41% for SO_4^{2-}. EC was also improved with ERA5, where NMB and NME changed from 141% to 133% and from - 38% to - 37%, respectively. However, OC was still under-predicted, especially on days with high OC concentrations, partly due to incomplete secondary organic aerosol treatment in the model, which included incomplete precursors and formation processes. EC predictions using ERA5 were slightly biased compared to the

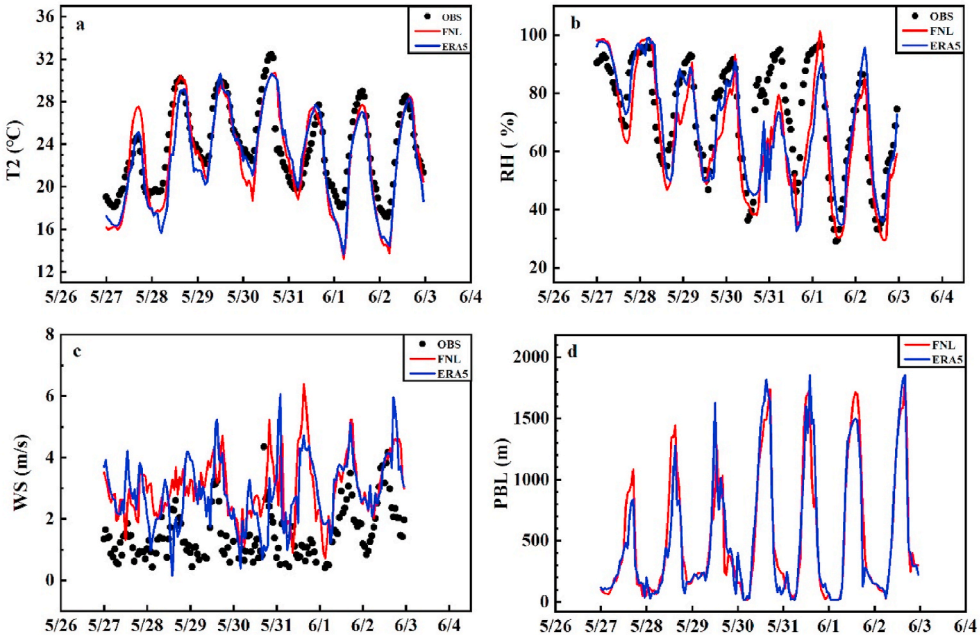

Fig. 6. Comparison of meteorological data and observations simulated using FNL and ERA5 meteorological data during 27 May to June 2, 2018 in Taizhou.

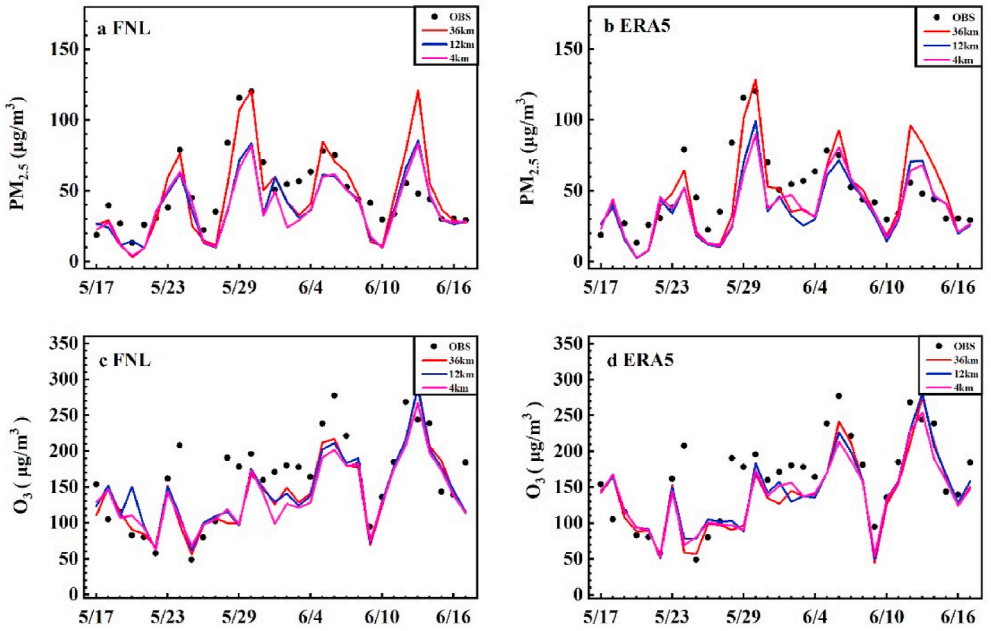

Fig. 7. Comparison of $PM_{2.5}$ (a, b) and MAD8h O_3 (c, d) resolution simulations using two kinds of meteorological data, FNL and ERA5, in Taizhou City from May to June 2018 (black dots represent observations; red lines represent the value of 36 km horizontal resolution; blue line indicates the value of 12 km horizontal resolution; purple line indicates the value of 4 km horizontal resolution). (For interpretation of the references to colour in this figure legend, the reader is referred to the Web version of this article.)

observations and predictions using FNL.

Specifically, CMAQ with the ERA reanalysis data captured the high $PM_{2.5}$ pollution event in Taizhou on 29–30 May 2018. The peak $PM_{2.5}$ observation equalled 120.25 μg/m^3. The predicted peak concentration with ERA5 was 89.99 μg/m^3, while it was 81.89 μg/m^3 with FNL.

To further analyse this event, Fig. 6 shows hourly T2, RH, WS, and PBL in Taizhou from 27 May to June 2, 2018 predicted with FNL and ERA5. Fig. 6 shows that the T2 predictions are similar during the event. The observed RH was nearly 100% during the early morning hours between 27 May and June 1, 2018. Both models under-predicted the high RH conditions on 29–31 May 2018, but ERA5 yielded slightly higher results than FNL. In addition, ERA5 predicted lower WS on 28–29 May 2018 compared to FNL. ERA5 also predicted lower PBL on 27–28 May 2018 compared to FNL.

$PM_{2.5}$ concentration predicted by ERA5 was higher than that predicted by FNL between 5 June and June 7, 2018. Fig. 2 shows the lower PBL values predicted by ERA5 during this period. Meanwhile, ERA5 predicted higher SO_4^{2-}, NO_3^-, and NH_4^+ concentrations during this period compared to FNL. Therefore, the lower PBL values predicted by ERA5 led to the higher concentrations of NO_3^-, SO_4^{2-}, and NH_4^+, while the lower predicted WS values by ERA5 on the days before May 30, 2018 accumulated the pollutants in the surface layer.

3.3. Impact of grid resolution on air quality predictions

Fig. 7 compares the predicted $PM_{2.5}$ and O_3-8 h acquired with the 36, 12, and 4 km grid resolutions. The results show that for both FNL and ERA5 reanalysis data, the model resolution had a negligible impact on

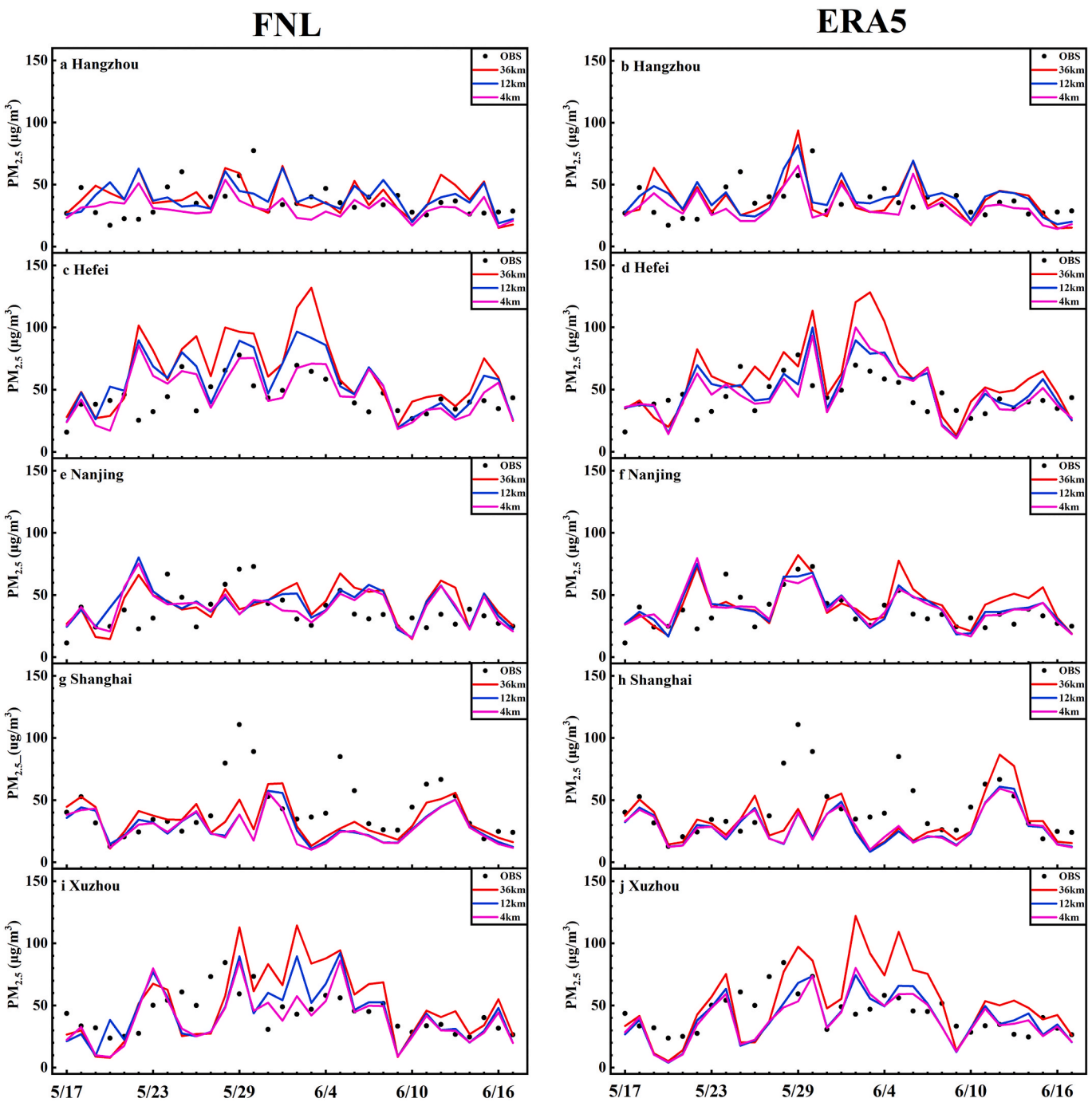

Fig. 8. Comparison of $PM_{2.5}$ resolution simulations using two kinds of meteorological data, FNL and ERA5, in 6 cities from May to June 2018 (black dots represent observations; red lines represent the value of 36 km horizontal resolution; blue line indicates the value of 12 km horizontal resolution; purple line indicates the value of 4 km horizontal resolution). (For interpretation of the references to colour in this figure legend, the reader is referred to the Web version of this article.)

the air quality predictions in Taizhou. Additionally, the $PM_{2.5}$ predictions at 36 km resolution agreed better with the observational data than those at 12 and 4 km. Therefore, a higher resolution does not always yield better predictions. In this study, the spatial resolution of the emission inputs was 25 × 25 km. Such a resolution is likely an important factor that affects model performance with higher grid resolutions. Figs. 8 and 9 show the impact of grid resolution on the $PM_{2.5}$ and O_3-8 h predictions in other YRD cities, similar to the findings in Taizhou.

4. Conclusions

In this study, we applied the WRF/CMAQ air quality modelling system to simulate air quality during the EXPLORE-YRD campaign. We used two different sets of reanalysis data—FNL and ERA5—to drive the model predictions. Model predictions were evaluated using the measured $PM_{2.5}$ composition data in Taizhou and other routine measurements of O_3 and $PM_{2.5}$ in the other key cities of the YRD region (i.e. Shanghai, Nanjing, Hangzhou, Hefei, and Xuzhou). We also discussed the impact of different meteorological reanalysis data and grid resolutions on CMAQ performance. The following conclusions were drawn from this study.

(1) $PM_{2.5}$ was generally under-predicted using the FNL and ERA5 datasets. ERA5 yielded slightly higher $PM_{2.5}$ predictions during

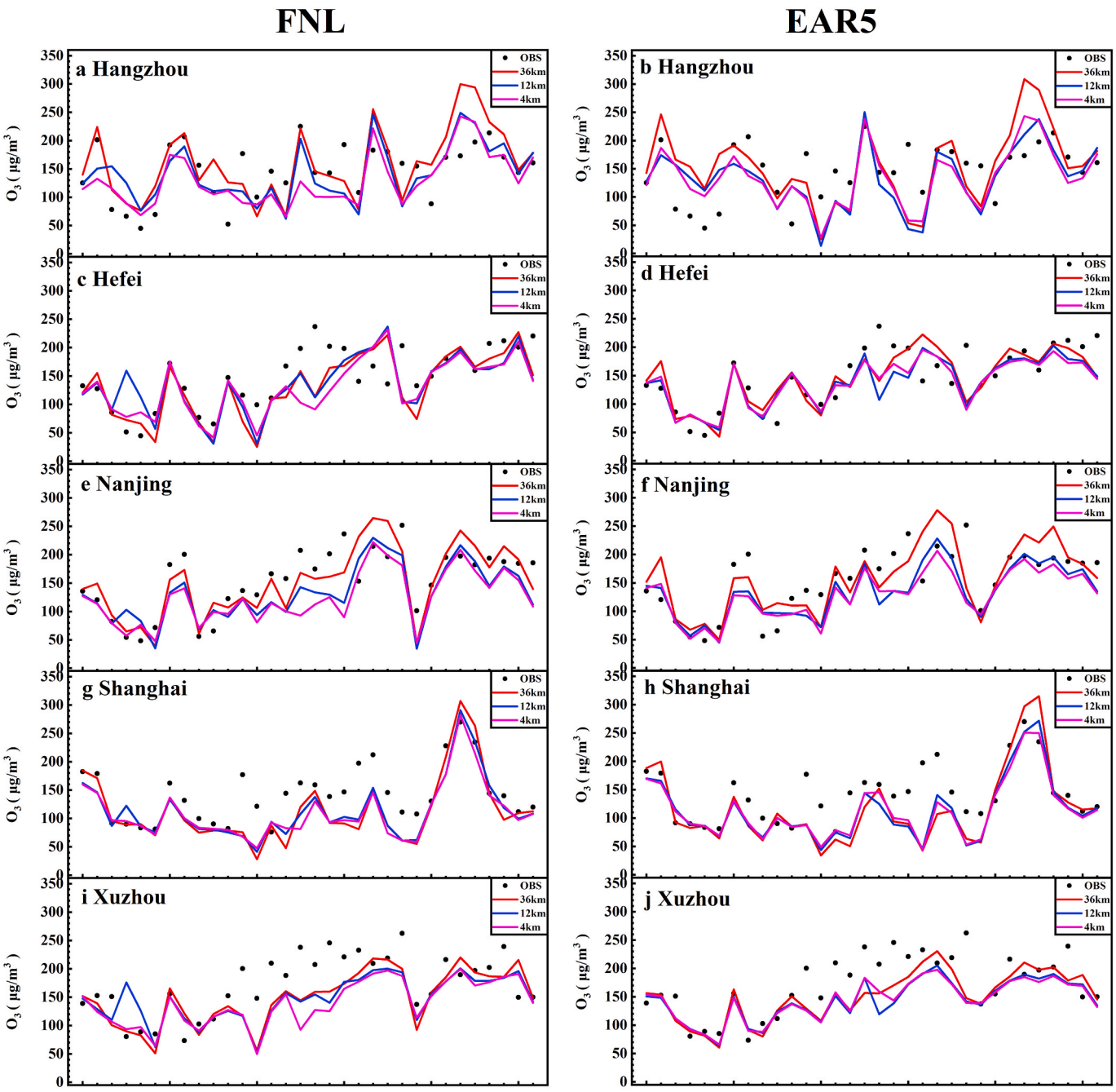

Fig. 9. Comparison of MAD8h O_3 resolution simulations using two kinds of meteorological data, FNL and ERA5, in 6 cities from May to June 2018 (black dots represent observations; red lines represent the value of 36 km horizontal resolution; blue line indicates the value of 12 km horizontal resolution; purple line indicates the value of 4 km horizontal resolution). (For interpretation of the references to colour in this figure legend, the reader is referred to the Web version of this article.)

the EXPLORE-YRD campaign. Both reanalysis data sets under-predicted the high $PM_{2.5}$ pollution processes from 29 to 30 May 2018, indicating that reanalysis data is not the key factor for under-predicting extreme $PM_{2.5}$ pollution processes. The performance of O_3 was similar in both sets of reanalysis data because O_3 is mostly sensitive to temperature predictions, and FNL and ERA5 yielded similar temperature results.

(2) Although the average performance of the $PM_{2.5}$ and O_3 predictions yielded by FNL and ERA5 was similar, significant differences were observed in certain locations on specific days (e.g. in Hangzhou from 29 May to June 6, 2018 and in Hefei from 1 to 3 June 2018). Therefore, the choice of reanalysis data affects the predictions of $PM_{2.5}$ and O_3. Model performance depends on study locations and episodes, and model performance evaluation is strongly suggested for model applications.

(3) Both the $PM_{2.5}$ and O_3 predictions were not very sensitive to the choice of model horizontal resolution (i.e. 36, 12, or 4 km), which can be partially explained by the same inventory with a resolution of 25 km used herein. Future studies should further investigate this issue when finer resolution emission inventory (e.g. 4 or 1 km) becomes available.

CRediT authorship contribution statement

Xueying Wang: Conceptualization, Data curation, Formal analysis, Writing - original draft. **Lin Li:** Data curation, Formal analysis, Writing -

review & editing. **Kangjia Gong:** Data curation, Formal analysis, Writing - review & editing. **Jianjiong Mao:** Data curation, Formal analysis, Writing - review & editing. **Jianlin Hu:** Conceptualization, Funding acquisition, Methodology, Writing - review & editing. **Jingyi Li:** Funding acquisition, Writing - review & editing, Methodology. **Zhenxin Liu:** Methodology, Writing - review & editing. **Hong Liao:** Writing - review & editing. **Wanyi Qiu:** Data curation, Writing - review & editing. **Ying Yu:** Data curation, Writing - review & editing. **Huabin Dong:** Data curation. **Song Guo:** Data curation, Writing - review & editing. **Min Hu:** Writing - review & editing. **Liming Zeng:** Writing - review & editing. **Yuanhang Zhang:** Writing - review & editing.

Declaration of competing interest

The authors declare that they have no known competing financial interests or personal relationships that could have appeared to influence the work reported in this paper.

Acknowledgement

This work was supported by the National Key R&D Program of China (2018YFC0213800), the National Natural Science Foundation of China (41975162, 41675125 and 41705102), and Jiangsu Environmental Protection Research Project (2016015).

Appendix A. Supplementary data

Supplementary data to this article can be found online at https://doi.org/10.1016/j.atmosenv.2020.118131.

References

Angevine, W.M., Eddington, L., Durkee, K., Fairall, C., Bianco, L., Brioude, J., 2012. Meteorological model evaluation for CalNex 2010. Mon. Weather Rev. 140, 3885–3906.

Arunachalam, S., Holland, A., Do, B., Abraczinskas, M., 2006. A quantitative assessment of the influence of grid resolution on predictions of future-year air quality in North Carolina, USA. Atmos. Environ. 40, 5010–5026.

(C3S), C.C.C.S., 2017. ERA5: Fifth Generation of ECMWF Atmospheric Reanalyses of the Global Climate . Copernicus Climate Change Service Climate Data Store (CDS), Date of Access.

Carter, W.P.L., Heo, G., 2012. Development of Revised SAPRC Aromatics Mechanisms. Final Report to the California Air Resources Board, Contracts No. 07-730 and 08-326. April 12, 2012.

Ding, D., Xing, J., Wang, S., Chang, X., Hao, J., 2019. Impacts of emissions and meteorological changes on China's ozone pollution in the warm seasons of 2013 and 2017. Front. Environ. Sci. Eng. 13.

Dong, H.B., Zeng, L.M., Hu, M., Wu, Y.S., Zhang, Y.H., Slanina, J., Zheng, M., Wang, Z.F., Jansen, R., 2012. Technical Note: the application of an improved gas and aerosol collector for ambient air pollutants in China. Atmos. Chem. Phys. 12, 10519–10533.

Emery, C., Tai, E., Yarwood, G., 2001. Enhanced meteorological modeling and performance evaluation for two Texas episodes. In: Internatioanl Corp (Ed.), Report to the Texas Natural Resources Conservation Commission, p.B.E. Novato, CA.

Emery, C., Liu, Z., Russell, A.G., Odman, M.T., Yarwood, G., Kumar, N., 2017. Recommendations on statistics and benchmarks to assess photochemical model performance. J. Air Waste Manag. Assoc. 67, 582–598.

Fan, H., Zhao, C., Yang, Y., 2020. A comprehensive analysis of the spatio-temporal variation of urban air pollution in China during 2014–2018. Atmos. Environ. 220, 117066.

Fast, J.D., Allan, J., Bahreini, R., Craven, J., Emmons, L., Ferrare, R., Hayes, P.L., Hodzic, A., Holloway, J., Hostetler, C., Jimenez, J.L., Jonsson, H., Liu, S., Liu, Y., Metcalf, A., Middlebrook, A., Nowak, J., Pekour, M., Perring, A., Russell, L., Sedlacek, A., Seinfeld, J., Setyan, A., Shilling, J., Shrivastava, M., Springston, S., Song, C., Subramanian, R., Taylor, J.W., Vinoj, V., Yang, Q., Zaveri, R.A., Zhang, Q., 2014. Modeling regional aerosol and aerosol precursor variability over California and its sensitivity to emissions and long-range transport during the 2010 CalNex and CARES campaigns. Atmos. Chem. Phys. 14, 10013–10060.

Gsella, A., de Meij, A., Kerschbaumer, A., Reimer, E., Thunis, P., Cuvelier, C., 2014. Evaluation of MM5, WRF and TRAMPER meteorology over the complex terrain of the Po Valley, Italy. Atmos. Environ. 89, 797–806.

Guenther, A.B., Jiang, X., Heald, C.L., Sakulyanontvittaya, T., Duhl, T., Emmons, L.K., Wang, X., 2012. The Model of Emissions of Gases and Aerosols from Nature version 2.1 (MEGAN2.1): an extended and updated framework for modeling biogenic emissions. Geosci. Model Dev. (GMD) 5, 1471–1492.

Guo, S., Hu, M., Zamora, M.L., Peng, J.F., Shang, D.J., Zheng, J., Du, Z.F., Wu, Z., Shao, M., Zeng, L.M., Molina, M.J., Zhang, R.Y., 2014. Elucidating severe urban haze formation in China. P Natl Acad Sci USA 111, 17373–17378.

Guo, S., Hu, M., Peng, J.F., Wu, Z.J., Zamora, M.L., Shang, D.J., Du, Z.F., Zheng, J., Fang, X., Tang, R.Z., Wu, Y.S., Zeng, L.M., Shuai, S.J., Zhang, W.B., Wang, Y., Ji, Y. M., Li, Y.X., Zhang, A.L., Wang, W.G., Zhang, F., Zhao, J.Y., Gong, X.L., Wang, C.Y., Molina, M.J., Zhang, R.Y., 2020. Remarkable nucleation and growth of ultrafine particles from vehicular exhaust. P Natl Acad Sci USA 117, 3427–3432.

Hersbach, H., Bell, B., Berrisford, P., Hirahara, S., Horányi, A., Muñoz-Sabater, J., Nicolas, J., Peubey, C., Radu, R., Schepers, D., Simmons, A., Soci, C., Abdalla, S., Abellan, X., Balsamo, G., Bechtold, P., Biavati, G., Bidlot, J., Bonavita, M., Chiara, G., Dahlgren, P., Dee, D., Diamantakis, M., Dragani, R., Flemming, J., Forbes, R., Fuentes, M., Geer, A., Haimberger, L., Healy, S., Hogan, R.J., Hólm, E., Janisková, M., Keeley, S., Laloyaux, P., Lopez, P., Lupu, C., Radnoti, G., Rosnay, P., Rozum, I., Vamborg, F., Villaume, S., Thépaut, J.N., 2020. The ERA5 global reanalysis. Q. J. R. Meteorol. Soc. 146, 1999–2049.

Hu, J., Ying, Q., Chen, J.J., Mahmud, A., Zhao, Z., Chen, S.H., Kleeman, M.J., 2010. Particulate air quality model predictions using prognostic vs. diagnostic meteorology in central California. Atmos. Environ. 44, 215–226.

Hu, W.W., Hu, M., Deng, Z.Q., Xiao, R., Kondo, Y., Takegawa, N., Zhao, Y.J., Guo, S., Zhang, Y.H., 2012. The characteristics and origins of carbonaceous aerosol at a rural site of PRD in summer of 2006. Atmos. Chem. Phys. 12, 1811–1822.

Hu, J., Wang, Y., Ying, Q., Zhang, H., 2014. Spatial and temporal variability of PM2.5 and PM10 over the North China plain and the Yangtze River delta, China. Atmos. Environ. 95, 598–609.

Hu, J., Zhang, H., Ying, Q., Chen, S.-H., Vandenberghe, F., Kleeman, M.J., 2015. Long-term particulate matter modeling for health effect studies in California - Part I: model performance on temporal and spatial variations. Atmos. Chem. Phys. 15, 3445–3461.

Hu, J., Chen, J., Ying, Q., Zhang, H., 2016a. One-year simulation of ozone and particulate matter in China using WRF/CMAQ modeling system. Atmos. Chem. Phys. 16, 10333–10350.

Hu, J., Chen, J., Ying, Q., Zhang, H., 2016b. One-year simulation of ozone and particulate matter in China using WRF/CMAQ modeling system. Atmos. Chem. Phys. 16, 10333–10350.

Hu, J., Huang, L., Chen, M., He, G., Zhang, H., 2017a. Impacts of power generation on air quality in China—Part II: future scenarios. Resour. Conserv. Recycl. 121, 115–127.

Hu, J., Wang, P., Ying, Q., Zhang, H., Chen, J., Ge, X., Li, X., Jiang, J., Wang, S., Zhang, J., Zhao, Y., Zhang, Y., 2017b. Modeling biogenic and anthropogenic secondary organic aerosol in China. Atmos. Chem. Phys. 17, 77–92.

Hu, J., Wang, P., Ying, Q., Zhang, H., Chen, J., Ge, X., Li, X., Jiang, J., Wang, S., Zhang, J., Zhao, Y., Zhang, Y., 2017c. Modeling biogenic and anthropogenic secondary organic aerosol in China. Atmos. Chem. Phys. 17, 77–92.

Hu, J.L., Li, X., Huang, L., Ying, Q., Zhang, Q., Zhao, B., Wang, S.X., Zhang, H.L., 2017d. Ensemble prediction of air quality using the WRF/CMAQ model system for health effect studies in China. Atmos. Chem. Phys. 17, 13103–13118.

Huang, C., Chen, C.H., Li, L., Cheng, Z., Wang, H.L., Huang, H.Y., Streets, D.G., Wang, Y. J., Zhang, G.F., Chen, Y.R., 2011. Emission inventory of anthropogenic air pollutants and VOC species in the Yangtze River Delta region, China. Atmos. Chem. Phys. 11, 4105–4120.

Jiang, X., Yoo, E.H., 2018. The importance of spatial resolutions of Community Multiscale Air Quality (CMAQ) models on health impact assessment. Sci. Total Environ. 627, 1528–1543.

Kang, H., Zhu, B., Gao, J., He, Y., Wang, H., Su, J., Pan, C., Zhu, T., Yu, B., 2019. Potential impacts of cold frontal passage on air quality over the Yangtze River Delta, China. Atmos. Chem. Phys. 19, 3673–3685.

Kota, S.H., Guo, H., Myllyvirta, L., Hu, J., Sahu, S.K., Garaga, R., Ying, Q., Gao, A., Dahiya, S., Wang, Y., Zhang, H., 2018. Year-long simulation of gaseous and particulate air pollutants in India. Atmos. Environ. 180, 244–255.

Li, H., Li, L., Huang, C., An, J.-y., Yan, R.-s., Huang, H.-y., Wang, Y.-j., Lu, Q., Wang, Q., Lou, S.-r., Wang, H.-l., Zhou, M., Tao, S.-k., Qiao, L.-p., Chen, M.-h., 2015a. Ozone source apportionment at urban area during a typical photochemical pollution episode in the summer of 2013 in the Yangtze River Delta. Huan jing ke xue= Huanjing kexue 36, 1–10.

Li, J., Cleveland, M., Ziemba, L.D., Griffin, R.J., Barsanti, K.C., Pankow, J.F., Ying, Q., 2015b. Modeling regional secondary organic aerosol using the Master Chemical Mechanism. Atmos. Environ. 102, 52–61.

Li, L., An, J.Y., Shi, Y.Y., Zhou, M., Yan, R.S., Huang, C., Wang, H.L., Lou, S.R., Wang, Q., Lu, Q., Wu, J., 2016. Source apportionment of surface ozone in the Yangtze River Delta, China in the summer of 2013. Atmos. Environ. 144, 194–207.

Li, L., An, J., Huang, L., Yan, R., Huang, C., Yarwood, G., 2019. Ozone source apportionment over the Yangtze River Delta region, China: investigation of regional transport, sectoral contributions and seasonal differences. Atmos. Environ. 202, 269–280.

Liu, J.-m., Wang, P.-f., Zhang, H.-l., Du, Z.-y., Zheng, B., Yu, Q.-q., Zheng, G.-j., Ma, Y.-l., Zheng, M., Cheng, Y., Zhang, Q., He, K.-b., 2020a. Integration of field observation and air quality modeling to characterize Beijing aerosol in different seasons. Chemosphere 242, 125195.

Liu, T., Wang, C., Wang, Y., Huang, L., Li, J., Xie, F., Zhang, J., Hu, J., 2020b. Impacts of model resolution on predictions of air quality and associated health exposure in Nanjing, China. Chemosphere 249, 126515.

Lu, K.D., Guo, S., Tan, Z.F., Wang, H.C., Shang, D.J., Liu, Y.H., Li, X., Wu, Z.J., Hu, M., Zhang, Y.H., 2019. Exploring atmospheric free-radical chemistry in China: the self-cleansing capacity and the formation of secondary air pollution. Natl Sci Rev 6, 579–594.

Ma, T., Duan, F., He, K., Qin, Y., Tong, D., Geng, G., Liu, X., Li, H., Yang, S., Ye, S., Xu, B., Zhang, Q., Ma, Y., 2019. Air pollution characteristics and their relationship with emissions and meteorology in the Yangtze River Delta region during 2014-2016. J. Environ. Sci. 83, 8–20.

Michelson, S.A., Djalalova, I.V., Bao, J.W., 2010. Evaluation of the summertime low-level winds simulated by MM5 in the central valley of California. J Appl Meteorol Clim 49, 2230–2245.

Ming, L., Jin, L., Li, J., Fu, P., Yang, W., Liu, D., Zhang, G., Wang, Z., Li, X., 2017. PM2.5 in the Yangtze River Delta, China: chemical compositions, seasonal variations, and regional pollution events. Environ. Pollut. 223, 200–212.

Monk, K., Guérette, E.-A., Paton-Walsh, C., Silver, J.D., Emmerson, K.M., Utembe, S.R., Zhang, Y., Griffiths, A.D., Chang, L.T.C., Duc, H.N., Trieu, T., Scorgie, Y., Cope, M.E., 2019. Evaluation of regional air quality models over Sydney and Australia: Part 1—meteorological model comparison. Atmosphere 10, 374.

Nguyen, G.T.H., Shimadera, H., Uranishi, K., Matsuo, T., Kondo, A., 2019. Numerical assessment of PM2.5 and O3 air quality in Continental Southeast Asia: impacts of potential future climate change. Atmos. Environ. 215, 116901.

Pan, S., Choi, Y., Roy, A., Jeon, W., 2017. Allocating emissions to 4 km and 1 km horizontal spatial resolutions and its impact on simulated NOx and O3 in Houston, TX. Atmos. Environ. 164, 398–415.

Pui, D.Y.H., Chen, S.-C., Zuo, Z., 2014. PM 2.5 in China: measurements, sources, visibility and health effects, and mitigation. Particuology 13, 1–26.

Ritter, M., Müller, M.D., Jorba, O., Parlow, E., Liu, L.J.S., 2012. Impact of chemical and meteorological boundary and initial conditions on air quality modeling: WRF-Chem sensitivity evaluation for a European domain. Meteorol. Atmos. Phys. 119, 59–70.

Shen, X.J., Sun, J.Y., Zhang, X.Y., Zhang, Y.M., Zhang, L., Che, H.C., Ma, Q.L., Yu, X.M., Yue, Y., Zhang, Y.W., 2015. Characterization of submicron aerosols and effect on visibility during a severe haze-fog episode in Yangtze River Delta, China. Atmos. Environ. 120, 307–316.

Shu, L., Xie, M., Wang, T., Gao, D., Chen, P., Han, Y., Li, S., Zhuang, B., Li, M., 2016. Integrated studies of a regional ozone pollution synthetically affected by subtropical high and typhoon system in the Yangtze River Delta region, China. Atmos. Chem. Phys. 16, 15801–15819.

Shu, L., Xie, M., Gao, D., Wang, T., Fang, D., Liu, Q., Huang, A., Peng, L., 2017. Regional severe particle pollution and its association with synoptic weather patterns in the Yangtze River Delta region, China. Atmos. Chem. Phys. 17, 12871–12891.

Shu, L., Wang, T., Xie, M., Li, M., Zhao, M., Zhang, M., Zhao, X., 2019. Episode study of fine particle and ozone during the CAPUM-YRD over Yangtze River Delta of China: characteristics and source attribution. Atmos. Environ. 203, 87–101.

Shu, L., Wang, T., Han, H., Xie, M., Chen, P., Li, M., Wu, H., 2020. Summertime ozone pollution in the Yangtze River Delta of eastern China during 2013-2017: synoptic impacts and source apportionment. Environ. Pollut. 257, 113631.

Tao, H., Xing, J., Zhou, H., Pleim, J., Ran, L., Chang, X., Wang, S., Chen, F., Zheng, H., Li, J., 2020. Impacts of improved modeling resolution on the simulation of meteorology, air quality, and human exposure to PM2.5, O3 in Beijing, China. J. Clean. Prod. 243, 118574.

Wang, Y., Ying, Q., Hu, J., Zhang, H., 2014. Spatial and temporal variations of six criteria air pollutants in 31 provincial capital cities in China during 2013–2014. Environ. Int. 73, 413–422.

Wang, M., Cao, C., Li, G., Singh, R.P., 2015. Analysis of a severe prolonged regional haze episode in the Yangtze River Delta, China. Atmos. Environ. 102, 112–121.

Wang, T., Xue, L., Brimblecombe, P., Lam, Y.F., Li, L., Zhang, L., 2017. Ozone pollution in China: a review of concentrations, meteorological influences, chemical precursors, and effects. Sci. Total Environ. 575, 1582–1596.

Wang, P., Guo, H., Hu, J., Kota, S.H., Ying, Q., Zhang, H., 2019a. Responses of PM2.5 and O3 concentrations to changes of meteorology and emissions in China. Sci. Total Environ. 662, 297–306.

Wang, R., Tie, X., Li, G., Zhao, S., Long, X., Johansson, L., An, Z., 2019b. Effect of ship emissions on O3 in the Yangtze River delta region of China: analysis of WRF-chem modeling. Sci. Total Environ. 683, 360–370.

Wang, Y., Zhao, Y., Zhang, L., Zhang, J., Liu, Y., 2020. Modified regional biogenic VOC emissions with actual ozone stress and integrated land cover information: a case study in Yangtze River Delta, China. Sci. Total Environ. 727, 138703.

Yang, X., Wu, Q., Zhao, R., Cheng, H., He, H., Ma, Q., Wang, L., Luo, H., 2019. New method for evaluating winter air quality: PM2.5 assessment using Community Multi-Scale Air Quality Modeling (CMAQ) in Xi'an. Atmos. Environ. 211, 18–28.

Ying, Q., Cureño, I.V., Chen, G., Ali, S., Zhang, H., Malloy, M., Bravo, H.A., Sosa, R., 2014. Impacts of Stabilized Criegee Intermediates, surface uptake processes and higher aromatic secondary organic aerosol yields on predicted PM2.5 concentrations in the Mexico City Metropolitan Zone. Atmos. Environ. 94, 438–447.

Ying, Q., Li, J., Kota, S.H., 2015. Significant contributions of isoprene to summertime secondary organic aerosol in eastern United States. Environ. Sci. Technol. 49, 7834–7842.

Yusoff, M.F., Latif, M.T., Juneng, L., Khan, M.F., Ahamad, F., Chung, J.X., Mohtar, A.A. A., 2019. Spatio-temporal assessment of nocturnal surface ozone in Malaysia. Atmos. Environ. 207, 105–116.

Zhang, H., Chen, G., Hu, J., Chen, S.-H., Wiedinmyer, C., Kleeman, M., Ying, Q., 2014. Evaluation of a seven-year air quality simulation using the Weather Research and Forecasting (WRF)/Community Multiscale Air Quality (CMAQ) models in the eastern United States. Sci. Total Environ. 473–474, 275–285.

Zhang, Q., Xue, D., Liu, X., Gong, X., Gao, H., 2019. Process analysis of PM2.5 pollution events in a coastal city of China using CMAQ. J. Environ. Sci. 79, 225–238.

Zhang, Y., Cao, Y., Tang, Y., Ying, Q., Hopke, P.K., Zeng, Y., Xu, X., Xia, Z., Qiao, X., 2020. Wet deposition of sulfur and nitrogen at Mt. Emei in the West China Rain Zone, southwestern China: status, inter-annual changes, and sources. Sci. Total Environ. 713, 136676.